Small-scale modification to the lensing kernel

Boryana Hadzhiyska,[1] David Spergel,[1,2] and Joanna Dunkley[1,3]
[1]Department of Astrophysical Sciences, Princeton University, Princeton, New Jersey 08540, USA
[2]Flatiron Institute, Simons Foundation, 162 Fifth Avenue, New York, New York 10010, USA
[3]Department of Physics, Princeton University, Princeton, New Jersey 08544, USA

(Received 9 November 2017; published 20 February 2018)

Calculations of the cosmic microwave background (CMB) lensing power implemented into the standard cosmological codes such as CAMB and CLASS usually treat the surface of last scatter as an infinitely thin screen. However, since the CMB anisotropies are smoothed out on scales smaller than the diffusion length due to the effect of Silk damping, the photons which carry information about the small-scale density distribution come from slightly earlier times than the standard recombination time. The dominant effect is the scale dependence of the mean redshift associated with the fluctuations during recombination. We find that fluctuations at $k = 0.01$ Mpc^{-1} come from a characteristic redshift of $z \approx 1090$, while fluctuations at $k = 0.3$ Mpc^{-1} come from a characteristic redshift of $z \approx 1130$. We then estimate the corrections to the lensing kernel and the related power spectra due to this effect. We conclude that neglecting it would result in a deviation from the true value of the lensing kernel at the half percent level at small CMB scales. For an all-sky, noise-free experiment, this corresponds to a $\sim 0.1\sigma$ shift in the observed temperature power spectrum on small scales ($2500 \lesssim l \lesssim 4000$).

DOI: 10.1103/PhysRevD.97.043521

I. INTRODUCTION

Density fluctuations along the line of sight distort the images of observed galaxies. This effect is generally known as gravitational lensing. By analyzing such distorted images, one can obtain a map of the lensing potential, which can then be related to the matter power spectrum at a given redshift. In the case of cosmic microwave background (CMB) photons, these lensing distortions encode information about the density fluctuations between the early universe at $z \approx 1100$ and the present-day Universe. We observe them in the CMB anisotropies as slight modifications to their statistical properties [1–3]. Over the past decade, cosmologists have measured the CMB lensing signal through both autocorrelations and cross-correlations with other density probes (e.g., cosmic infrared background, galaxy lensing, galaxy counts, 21 cm probes) [3–8]. Lensing measurements can put constraints on the nature of dark energy and the expansion history of the Universe [9–11].

Lower-redshift information can be inferred from weak lensing studies, which measure the distortions of the shapes of galaxies caused by lensing. In both cases, the goal is to reconstruct the convergence field, which can be directly related to the projected matter density by measuring the magnification and shear effects from either distribution [12]. Since the lensing reconstruction information is encoded mostly in the smallest scales observed, high resolution and sensitivity are crucial for such measurements [13].

With the improvement in sensitivity expected in future experiments [14–16], it is becoming increasingly more important to take into consideration corrections to the observed power spectra, which have until now been negligible. One such effect comes from the fact that on scales smaller than the diffusion length, the density anisotropies are smoothed out due to photon diffusion damping. This means that photons carrying small-scale information need to have come from slightly earlier times than the standard recombination time [17,18]. The dominant effect is the scale dependence of the mean redshift associated with the fluctuations during recombination.

The standard calculation of the CMB lensing power implemented into numerical codes such as CAMB [19] and CLASS [20] treats the surface of last scatter as an infinitely thin screen. In this paper, we provide a modified estimation of the distance to last scattering as a function of scale. This correction takes into account the scale dependence of the recombination redshift in the calculation of the lensing kernel, which is needed to obtain the lensing power spectrum. We finally evaluate the percentage difference in the lensing kernel resulting from this modification and discuss its significance given the expected sensitivity of future experiments.

II. EFFECT ON LENSING KERNEL

The weighted projection of the matter density contrast δ, known as the convergence field, encodes information about

the density fluctuations in the Universe since the period of recombination and is expressed as

$$\kappa(\hat{n}) = \int_0^\infty dz W^\kappa(z)\delta(\chi(z)\hat{n}, z), \tag{1}$$

where $\chi(z)$ is the conformal distance between us and some event at redshift z [21]. In a flat universe, the lensing kernel W^κ is given by

$$W^\kappa(z) = \frac{3}{2}\Omega_m H_0^2 \frac{1+z}{H(z)}\frac{\chi(z)}{c}\int_z^\infty dz_s p_s(z_s)\frac{\chi(z_s)-\chi(z)}{\chi(z_s)}, \tag{2}$$

where $p_s(z)$ is the normalized distribution of sources as a function of redshift.

In the case of the CMB, it is standard to assume that the photons come predominantly from the redshift of recombination $z(\eta_*) \equiv z_*$, so that one can approximate the source distribution as $p_s \approx \delta_D(z - z_*)$ and thus obtain the kernel [12]:

$$W^\kappa(z) = \frac{3}{2}\Omega_m H_0^2 \frac{1+z}{H(z)}\frac{\chi(z)}{c}\frac{\chi(z_*)-\chi(z)}{\chi(z_*)}. \tag{3}$$

We, thus, see that the usual approach for calculating the lensing kernel, also employed by the cosmological codes CLASS and CAMB, treats the surface of last scatter as an infinitely thin screen. However, the CMB photons come from a range of redshifts which peaks at the period of recombination. The photons which last scattered at earlier times contain more small-scale information than those coming from later times because as the diffusion damping scale increases with time, anisotropies are smoothed out and information on small scales is lost [17,18]. The main effect is that the mean redshift associated with the fluctuations during recombination becomes scale dependent. This effect is illustrated in Fig. 1.

This claim can be supported quantitatively by considering the visibility function $v(\eta)$, which expresses the most probable time at which a CMB photon last scattered, and the damping factor $\exp[-k^2/k_D(\eta)^2]$, which measures how much the growth of a given mode is suppressed as a function of time [22]. Their product, computed for each mode, informs us about the most likely time at which the photons encoding information on the given mode last scattered:

$$g(k,\eta) = e^{-k^2/k_D(\eta)^2} v(\eta). \tag{4}$$

As seen in the lowest panel in Fig. 2, for small-scale modes, the product between the visibility function and the damping factor peaks at earlier times than the standard recombination time η_*, which shows that the CMB photons providing information on small-scale anisotropies

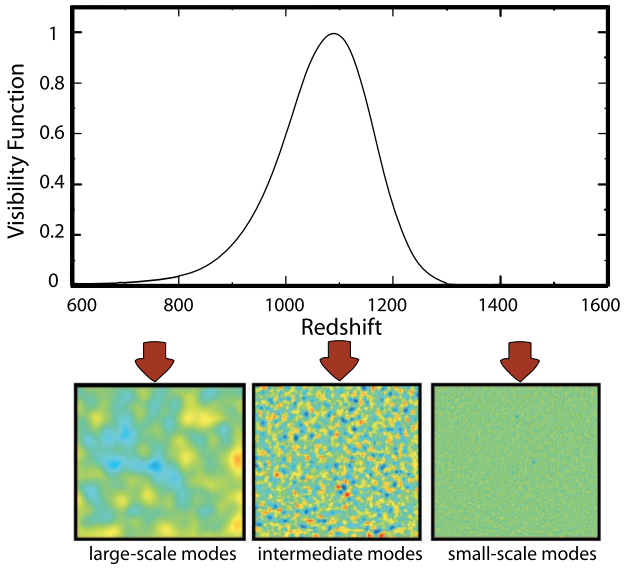

FIG. 1. The CMB anisotropies can be broken into small scale, intermediate scale and large scale. Due to diffusion damping, the small-scale information is provided by photons which last scattered at redshifts larger than the redshift of recombination. In contrast, at smaller redshifts, the information on small scales is lost, and large-scale information is provided by late-time photons.

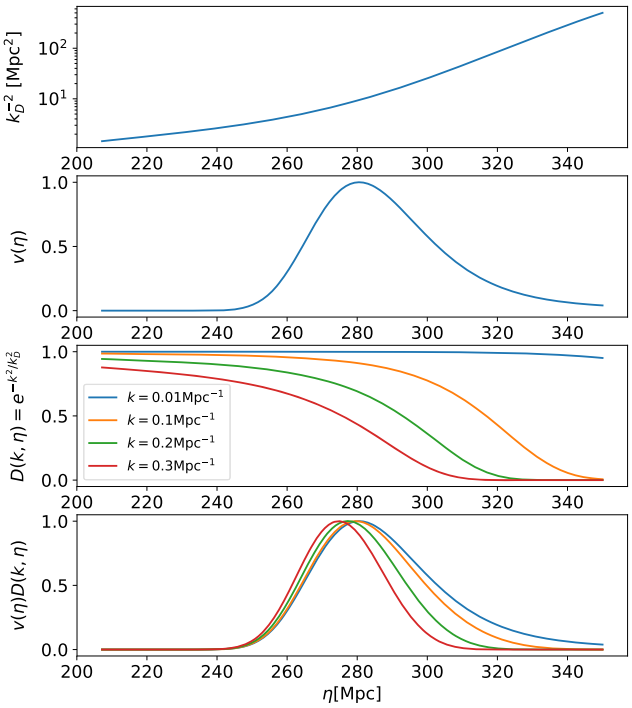

FIG. 2. Top two panels: Damping scale and visibility function as a function of conformal time. Bottom two panels: Damping factor and the normalized product between the damping factor and the visibility function for different wave numbers k. Smaller-scale modes are most likely to have scattered at earlier times.

($k \gtrsim 0.1$ Mpc^{-1}) are more likely to have come from an earlier time than the mean recombination time. On even smaller scales ($k \gtrsim 0.3$ Mpc^{-1}), where the primary anisotropies are washed out, the effective emission time is shifted to later times, as the motion of the photon-baryon fluid starts to be dominated by its infall into the CDM potential wells during matter domination. In this regime, the approximation which we are adopting breaks down and more careful analysis is needed. However, since we are interested in the effect on the temperature and the polarization power spectra for $l \lesssim 4000$, we can neglect the baryon effect.

A plot of conformal time $\eta_*(k)$ [Mpc] versus wave number k [Mpc^{-1}] obtained by numerically computing the peak position for each mode is shown in Fig. 3. We fit a cubic polynomial to this function, finding the form:

$$\eta_*(k) = -2.14[\ln(k)]^4 - 15.67[\ln(k)]^3 - 42.46[\ln(k)]^2 - 50.77[\ln(k)] + 257.76. \quad (5)$$

We can now incorporate the scale dependence of $\eta_*(k)$ into the kernel and obtain its form as a function of both redshift and CMB scale k, assuming that for each k, the source distribution can be approximated by $p_s \approx \delta_D(\eta - \eta_*(k))$:

$$W^\kappa(z,k) = \frac{3}{2}\Omega_m H_0^2 \frac{1+z}{H(z)} \frac{\chi(z)}{c} \frac{\chi(z_*,k) - \chi(z)}{\chi(z_*,k)}. \quad (6)$$

We show the impact on the lensing kernel as a function of CMB scale (k) in three panels (Fig. 4), each of which is a snapshot at a given redshift: $z = 1$, $z = 5$, and $z = 10$, respectively. One sees that the fractional difference is increasing approximately linearly with k due to the fact that the largest deviations of $\eta_*(k)$ from the standard value arise at the smaller scales ($k \sim 0.3$ Mpc^{-1}). Another observation is that the deviation from the standard value of the kernel increases with redshift: at redshift $z = 1$, the fractional difference is merely 0.01% on small scales, but it reaches 0.1% for redshift $z = 10$.

Using the Limber approximation [23,24], the modified equation for the power spectrum of the convergence field due to CMB lensing becomes

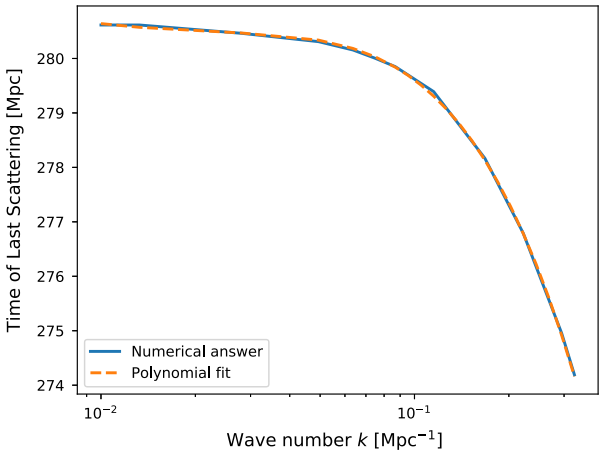

FIG. 3. Time of the last scattering of photons as a function of CMB scale. The blue curve is derived numerically by computing the peak of the product $g(k,\eta) = D(k,\eta)v(\eta)$ for each wave number k. The orange curve uses our approximate result from Eq. (4).

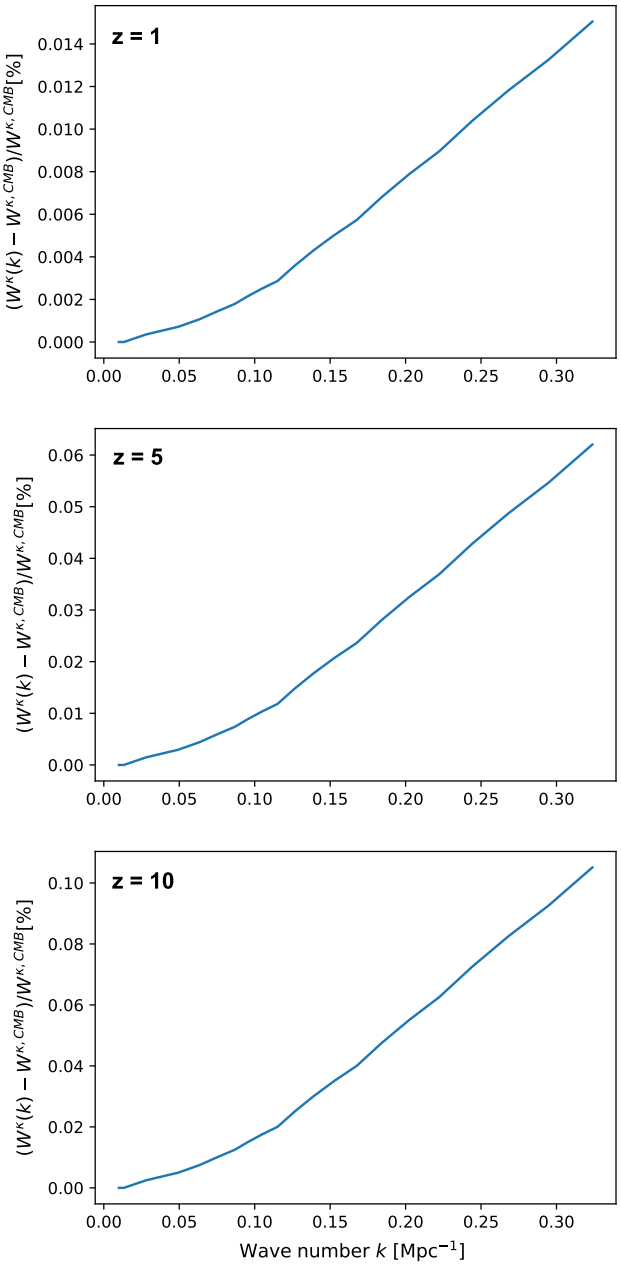

FIG. 4. Fractional difference in the lensing kernel at redshifts $z = 1$, $z = 5$ and $z = 10$ assuming that the distance to last scattering depends on the CMB scale k. The deviations from the standard value of the kernel increase with redshift and decrease with scale.

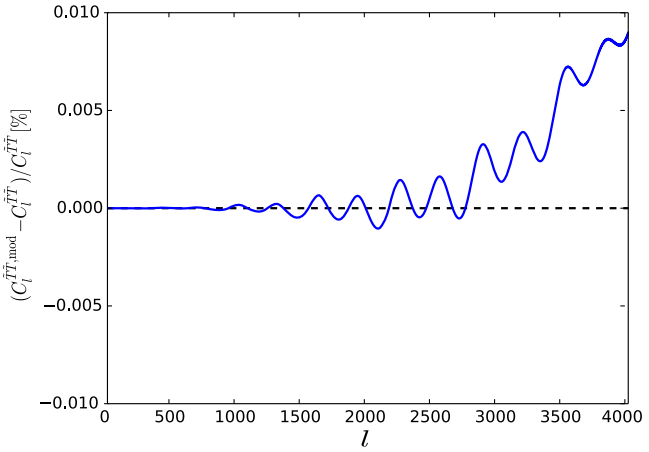

FIG. 5. Percentage difference in the lensed temperature power spectrum assuming a scale-dependent distance to last scattering. This result is derived by using the full-sky nonperturbative approximation in Ref. [25] to second order.

$$C^{\kappa\kappa}_{l,l'} = \int_0^\infty \frac{dz}{c}\frac{H(z)}{\chi(z)^2} W^\kappa(z, k' = l'/\chi_*)^2 P(k = l/\chi, z), \quad (7)$$

where χ_* is the mean distance to the last scattering surface. Note that in contrast with the standard calculation, here the lensing power spectrum depends on the two scales l (k) and l' (k'). Thus, $C^{\kappa\kappa}_{l,l'}$ effectively describes how much our signal will be lensed for a lens of size l (k) and a given size of the CMB anisotropy l' (k').

Since we expect very high sensitivity in the future measurements of the temperature power spectrum, an interesting observable to consider is the lensed temperature power spectrum $C_l^{\tilde{T}\tilde{T}}$, which is approximately given by the following modified equation:

$$C_l^{\tilde{T}\tilde{T}} \approx \int \frac{d^2\mathbf{l}'}{(2\pi)^2}\frac{4[\mathbf{l}'\cdot(\mathbf{l}-\mathbf{l}')]^2}{|\mathbf{l}-\mathbf{l}'|^4} C^{\kappa\kappa}_{|\mathbf{l}-\mathbf{l}'|,l'} C^{TT}_{l'} + C^{TT}_l\left[1 - \frac{1}{\pi}l^2\int\frac{dl'}{l'}C^{\kappa\kappa}_{l',l}\right]. \quad (8)$$

The resulting fractional difference in the temperature power spectrum is shown in Fig. 5, where we use a full-sky nonperturbative approximation [25]. As we increase l' and thus the distance to the source (small scales come from earlier times), the overall amplitude of the difference also gets larger, as expected in lensing theory. The average percentage difference across the small-scale modes $2500 \lesssim l \lesssim 4000$ is 0.004%. Consequently, the measured temperature power spectrum in an idealized all-sky, noise-free experiment with a signal-to-noise ratio of ≈2200 on these scales would be shifted by $\sim 0.1\sigma$ from the theoretically predicted one.

The corresponding equation for the lensed B-mode polarization power spectrum is

$$C_l^{\tilde{B}\tilde{B}} \approx \int \frac{d^2\mathbf{l}'}{(2\pi)^2}\frac{4[\mathbf{l}'\cdot(\mathbf{l}-\mathbf{l}')]^2}{|\mathbf{l}-\mathbf{l}'|^4}\sin^2(2\phi_{\mathbf{l},\mathbf{l}'}) C^{\kappa\kappa}_{|\mathbf{l}-\mathbf{l}'|,l'} C^{EE}_{l'}. \quad (9)$$

Since the B-mode power spectrum gives us a direct probe of the lensing amplitude, the resulting fractional difference is larger than in the case of temperature, peaking at roughly $l \approx 3000$ with $\Delta C_l^{\tilde{B}\tilde{B}}/C_l^{\tilde{B}\tilde{B}} \approx 0.03\%$. However, this deviation would be harder to measure in the near future due to the lower sensitivity of the polarization measurements compared with the temperature.

III. CONCLUSION

The smaller-scale anisotropies observed in the CMB come from slightly earlier times, which implies that the time of photon last scattering is dependent on the physical scale. This has important implications for the lensing kernel used to compute the observable power spectra. We found differences in the lensing kernel of ∼0.1% at redshift $z = 10$ and of ∼0.06% at redshift $z = 5$ for the smaller scales ($k \sim 0.3$ Mpc^{-1}). Consequently, this leads to an average deviation of 0.004% in the temperature power spectrum on small scales $2500 \lesssim l \lesssim 4000$. In the future, experiments will ideally only be limited by cosmic variance and will thus measure the temperature power spectrum with a signal-to-noise ratio of ≈2200 on scales $2500 \lesssim l \lesssim 4000$. Neglecting the scale dependence of recombination then would lead to a measurable deviation from the predicted power spectrum of about $\sim 0.1\sigma$ on these scales. An observable for which we expect the effect to be more prominent in the near future is the reconstructed lensing power spectrum, as it depends on the 4-point function of the lensed temperature map. We are hoping to look into it in a future paper. In the current age of precision cosmology, implementing such subpercent modifications to the observable power spectra is becoming increasingly important.

ACKNOWLEDGMENTS

We would like to thank Mathew S. Madhavacheril for providing us with useful lensing computational tools. We are further grateful to Antony Lewis, Anthony Challinor and Blake Sherwin for pointing out and discussing an inaccuracy in our application of the effect to CMB lensing. B. H. would like to thank the Department of Astrophysical Sciences at Princeton for the immense support during her undergraduate degree.

[1] U. Seljak, Astrophys. J. **463**, 1 (1996).
[2] W. Hu, Phys. Rev. D **62**, 043007 (2000).
[3] M. Zaldarriaga, Phys. Rev. D **62**, 063510 (2000).
[4] K. M. Smith, O. Zahn, and O. Doré, Phys. Rev. D **76**, 043510 (2007).
[5] L. E. Bleem *et al.*, Astrophys. J. Lett. **753**, L9 (2012).
[6] C. Feng, G. Aslanyan, A. V. Manohar, B. Keating, H. P. Paar, and O. Zahn, Phys. Rev. D **86**, 063519 (2012).
[7] B. D. Sherwin *et al.*, Phys. Rev. D **86**, 083006 (2012).
[8] P. A. R. Ade, N. Aghanim, M. Arnaud, M. Ashdown, J. Aumont, C. Baccigalupi, A. J. Banday, R. B. Barreiro, J. G. Bartlett *et al.* (Planck Collaboration), Astron. Astrophys. **594**, A15 (2016).
[9] W. Hu, Astrophys. J. **522**, L21 (1999).
[10] R. de Putter, O. Zahn, and E. V. Linder, Phys. Rev. D **79**, 065033 (2009).
[11] S. Das, R. de Putter, E. V. Linder, and R. Nakajima, J. Cosmol. Astropart. Phys. 11 (2012) 011.
[12] A. Lewis and A. Challinor, Phys. Rep. **429**, 1 (2006).
[13] D. Munshi, P. Valageas, L. van Waerbeke, and A. Heavens, Phys. Rep. **462**, 67 (2008).
[14] M. D. Niemack *et al.*, Proc. SPIE Int. Soc. Opt. Eng. **7741**, 77411S (2010).
[15] J. E. Austermann *et al.*, in Millimeter, Submillimeter, and Far-Infrared Detectors and Instrumentation for Astronomy VI, *Proc. SPIE*, Vol. 8452 (SPIE-International Society for Optical Engineering, Bellingham, WA, 2012), p. 84521E.
[16] K. Arnold *et al.*, Proc. SPIE Int. Soc. Opt. Eng. **7741**, 77411E (2010).
[17] J. Silk, Astrophys. J. **151**, 459 (1968).
[18] P. J. E. Peebles and J. T. Yu, Astrophys. J. **162**, 815 (1970).
[19] A. Lewis and A. Challinor, CAMB: Code for Anisotropies in the Microwave Background, Astrophysics Source Code Library, 2011, http://ascl.net/1102.026.
[20] D. Blas, J. Lesgourgues, and T. Tram, J. Cosmol. Astropart. Phys. 07 (2011) 034.
[21] M. Bartelmann and P. Schneider, Phys. Rep. **340**, 291 (2001).
[22] W. T. Hu, Ph.D. thesis, University of California, Berkeley, 1995, arXiv:astro-ph/9508126.
[23] D. N. Limber, Astrophys. J. **119**, 655 (1954).
[24] N. Kaiser, Astrophys. J. **388**, 272 (1992).
[25] A. Challinor and A. Lewis, Phys. Rev. D **71**, 103010 (2005).